ACS APPLIED MATERIALS & INTERFACES

Research Article

www.acsami.org

Availability of the Basal Planes of Graphene Oxide Determines Whether It Is Antibacterial

Liwei Hui,[†,‡] Ji-Gang Piao,[§,∥,#] Jeffrey Auletta,[⊥,#] Kan Hu,[†,‡,#] Yanwu Zhu,[†,‡] Tara Meyer,[⊥] Haitao Liu,*[,⊥] and Lihua Yang*[,‡,§,∥]

[†]CAS Key Laboratory of Materials for Energy Conversion, [‡]Department of Materials Science and Engineering, [§]CAS Key Laboratory of Soft Matter Chemistry, and [∥]Department of Polymer Science and Engineering, University of Science and Technology of China, 96 Jinzhai Road, Hefei, Anhui 230026, China

[⊥]Department of Chemistry, University of Pittsburgh, Pittsburgh, Pennsylvania 15260, United States

Supporting Information

ABSTRACT: There are significant controversies on the antibacterial properties of graphene oxide (GO): GO was reported to be bactericidal in saline, whereas its activity in nutrient broth was controversial. To unveil the mechanisms underlying these contradictions, we performed antibacterial assays under comparable conditions. In saline, bare GO sheets were intrinsically bactericidal, yielding a bacterial survival percentage of <1% at 200 μg/mL. Supplementing saline with ≤10% Luria−Bertani (LB) broth, however, progressively deactivated its bactericidal activity depending on LB-supplementation ratio. Supplementation of 10% LB made GO completely inactive; instead, ∼100-fold bacterial growth was observed. Atomic force microscopy images showed that certain LB components were adsorbed on GO basal planes. Using bovine serum albumin and tryptophan as well-defined model adsorbates, we found that noncovalent adsorption on GO basal planes may account for the deactivation of GO's bactericidal activity. Moreover, this deactivation mechanism was shown to be extrapolatable to GO's cytotoxicity against mammalian cells. Taken together, our observations suggest that bare GO intrinsically kills both bacteria and mammalian cells and noncovalent adsorption on its basal planes may be a global deactivation mechanism for GO's cytotoxicity.

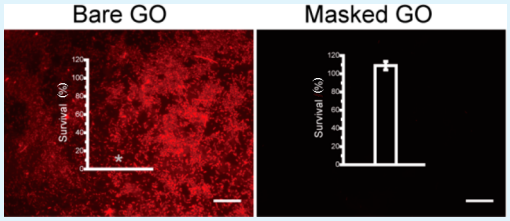

KEYWORDS: *graphene, antimicrobial, adsorption, mechanism, cytotoxicity*

INTRODUCTION

Graphene is an isolated single atomic layer of graphite—a free-standing one-atom-thick sheet of hexagonally arranged sp^2-bonded carbon atoms.[1] As the first two-dimensional (2D) atomic crystal ever available, graphene and graphene-derived materials have attracted tremendous attention from scientific communities in recent years.[1,2] Among them, graphene oxide (GO)—graphene sheets derivatized with carbonyl, epoxy, and hydroxyl functional groups[3]—is the most notable one.[4] Owing to the presence of these functional groups, GO can be readily dispersed in water, which made it a popular target for biomedical applications, as reviewed elsewhere.[4−6]

There are a number of investigations on the potential of GO as an antimicrobial. Their results are, however, contradictory. In classic bacterial killing assays, GO nanosheets dispersed in saline demonstrated definitive antibacterial activity.[7−11] After 2 h incubation with GO nanosheets of 85 μg/mL, 98.5% of treated *Escherichia coli*—a representative Gram-negative bacteria—cells were killed.[8] An increase in incubation time, GO dose, or average lateral-dimension of GO sheets generally led to increased potency of GO against *E. coli*.[9,12] Similarly, *Staphylococcus aureus*—a representative Gram-positive bacteria—can be killed by GO with comparable potency. After 1 h incubation with GO of the same dose in saline, only 41% and 26% of treated *E. coli* and *S. aureus* cells survived, respectively.[7] Similar bactericidal activity was observed with GO dispersed in deionized (DI) water.[13] Moreover, GO was reported to retain the antibacterial activity even when being formatted into free-standing GO-based papers[8,14] and nanocomposites complexed with other antibacterial agents.[15,16]

In contradiction with the definitive bactericidal activity of GO dispersed in saline and DI water, GO dispersed in nutrient broth was reported to exhibit controversial antibacterial activities. One study reported that GO in Luria−Bertani (LB) broth enhanced bacterial growth.[17] After 16 h incubation in LB broth, *E. coli* cells treated with 20 μg/mL GO achieved an optical density at 600 nm (OD_{600})—a turbidity parameter widely used to indicate bacterial growth—of 1.7, whereas those treated without GO only achieved an OD_{600} of 1.3; quantitative real-time PCR (qPCR) assays showed that *E. coli* cells treated with GO exhibited a higher number of bacterial genomic DNA copies than those treated without GO.[17] In stark contrast, some other studies reported that GO dispersed in LB broth inhibited bacterial growth.[11,18] During a 15 h incubation, *Pneumococcus*

Received: May 18, 2014
Accepted: July 4, 2014
Published: July 4, 2014

aeruginosa—a representative Gram-negative bacteria—treated with 75 μg/mL GO exhibited limited growth (OD_{600} < 0.2), whereas those treated without GO exhibited consistent growth (as indicated by the monotonically increasing OD_{600}, which eventually reached a maximum of ~1.2).[11] Another study even showed that GO exhibited a minimum inhibition concentration (MIC) of <1 μg/mL against both Gram-negative and -positive bacteria, according to turbidity, OD_{590}, measurements.[18] Differing from both stands above, one study reported that GO in trypticase soy broth (TSB)—one nutrient broth—imposed no significant effects on bacterial growth, as indicated by the close counts of colony-forming units (cfu) of bacteria treated with and without GO.[19] These contradictory results suggest an unknown mechanism affecting the antibacterial activity of GO; unfortunately, these studies used very different experimental conditions and evaluated different antibacterial properties (e.g., killing assay vs growth inhibition assay), making it difficult to correlate the results.

In this work, we systematically examined whether GO is intrinsically antibacterial and, if so, why the antimicrobial property appears to be controversial under certain conditions. Our study not only explains the contradictory results in the literature but also defines the necessary parameters for achieving the optimal bactericidal activity of GO.

MATERIALS AND METHODS

Graphene oxide (GO) sheets were prepared by bath-sonicating GtO particles prepared via a modified Hummers' method.[20,21] To assess whether GO is bactericidal and, if that is the case, why it exhibited contraversial antibacterial activity in nutrient broth, we performed classic plate killing assays using GO dispersions in both saline (0.9% NaCl) and LB-supplemented saline, with *E. coli* (ATCC 25922) used as a representative bacteria strain. In addition, comparable plate killing assays were performed using GO dispersions in saline supplemented with bovine serum albumin (BSA) and tryptophan—two well-defined adsorbates that GO basal planes readily adsorb—to evaluate how noncovalent adsorption on GO basal planes affects its antibacterial activity. The morphology and thickness of GO sheets in various dispersions were characterized using atomic force microscopy (AFM). Statistical comparisons were performed via Student's *t* test. To distinguish whether GO indeed kills bacteria or simply renders them unable to form visible colonies, we further performed fluorescence-microscopy-based bacterial dead/live viability assays using *E. coli* (ATCC 25922) and *B. subtilis* (ATCC 6051) as representive Gram-negative and -positive bacterial strains, respectively. Similar cell viability assays were performed against HepG2 cells, representative mammalian cells, to assess whether the deactivation mechanism of GO's antibacterial activity could be extrapolated to its cytotoxicity against mammalian cells. More experimental details and related information are described in the Supporting Information.

RESULTS AND DISCUSSION

As we briefly reviewed above, GO sheets dispersed in saline have demonstrated definitive bactericidal activity based on classic killing assay results,[7−10] indicating that GO is antibacterial. In contrast, GO sheets exhibited enhancive,[17] inhibitive,[11,18] or inactive[19] effects on the bacterial growth in growth inhibition assays, indicating that GO has contradictory antibacterial properties. It should be noted that these two types of antibacterial assays differ in both their experimental conditions and the antibacterial property they evaluate. A bacteria killing assay is normally performed in buffer or saline, which lack the necessary nutrients to support bacterial growth and evaluates the effects on bacteria viability, whereas a growth inhibition assay is normally performed in nutrient broth and evaluates the effects on bacterial growth. Such difference may account for the contradictory results on whether GO is antibacterial.

To elucidate the mechanisms underlying the controversial antibacterial property of GO, it is critical to perform antibacterial assays under comparable conditions and evaluate the same antibacterial property. Note that OD_{600} readings of mixtures of GO sheets, nutrient broth, and/or bacterial cells were significantly larger than the sum of the OD_{600} of the constituents (Figure S3, Supporting Information).We believe that this observation is due to the colloidal instability of GO sheets in the presence of nutrient broth and/or bacterial cells; the aggregated GO scatters light and results in an anomalously large OD_{600} reading. As a result, OD_{600}, though widely used to indicate bacterial growth in bacterial growth inhibition assays, may falsely indicate bacterial growth in the presence of GO. Having these concerns in mind, we turned to bactericidal assays and compared the bactericidal activity of GO in both unmodified saline and broth-supplemented saline.

To determine whether GO is antibacterial, we first assessed its bactericidal activity in saline. Freshly prepared GO dispersion in saline at 200 μg/mL appeared optically clear and light brown. The dispersion was stable and little or no agglomeration/precipitation was observed after standing still for 4 h (Figure 1a). Atomic force microscopy (AFM)

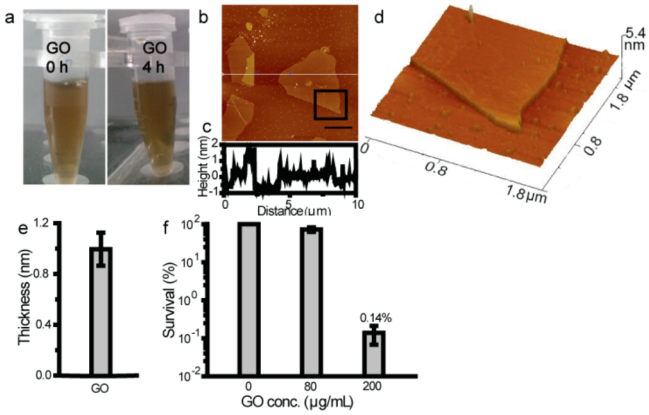

Figure 1. GO dispersion in saline and related characterizations. (a) Photographs of GO dispersion in saline at 200 μg/mL before (left) and after (right) standing for 4 h. (b) A representative AFM image of GO sheets and the corresponding (c) height and (d) three-dimensional profiles. Scale bar = 2 μm. On the basis of the height profiles of AFM images, (e) GO sheets in saline have an average sheet thickness of 1.00 ± 0.13 nm (averaged over seven individual sheets), indicative of a monolayer of bare GO sheets. (f) Plate killing assays against *E. coli* using GO sheets of 80 and 200 μg/mL in saline. Controls were samples assayed in comparable ways but in the absence of GO and are marked as 0 μg/mL GO. The *E. coli* inoculation level was ~5×10^5 cfu/mL. The difference in survival percentages between bacterial cells treated with 80 μg/mL GO and control has $p > 0.05$, whereas that between cells treated with 200 μg/mL GO and control has $p < 0.01$. Data points are reported as mean ± standard deviation.

characterizations (Figure 1b−d) showed that the as-prepared GO exhibited flat-sheet morphology and, on the basis of the corresponding height profiles (Figure 1c), had an average thickness of 1.00 ± 0.13 nm (n = 7, Figure 1e), indicative of monolayer bare GO sheets. To evaluate whether our GO sheets in saline are bactericidal, we performed classic plate killing assays using *E. coli* (ATCC 25922) as a representative bacterial

strain. After 3 h incubation, GO sheets of 80 and 200 μg/mL resulted in bacterial survival percentages of 72.7% and 0.14%, respectively (Figure 1f). Statistical comparisons using Student's *t* test analysis revealed that the difference in survival percentage between samples treated with 200 μg/mL GO and controls had $p < 0.01$, indicative of a statistically significant difference, as compared to $p > 0.05$ for samples treated with 80 μg/mL GO and controls. Therefore, we used 200 μg/mL as GO dose for all the following experiments unless specified otherwise. Obviously, our plate killing assays indicate that GO is bactericidal, which is consistent with previous assays conducted in saline.[7−11]

To evaluate the bactericidal activity of GO in the presence of LB nutrients, we supplemented saline with trace amounts of LB broth, ≤10% (volume ratio, v/v), and performed the same bactericidal assays that we had performed on the GO dispersions in unmodified saline. The differences were striking. Freshly prepared GO dispersion in LB-supplemented saline (5%, LB broth) appeared to be clear and light brown in color, similar to GO in saline, but agglomeration and slight precipitation occurred after standing still for 4 h (Figure 2a).

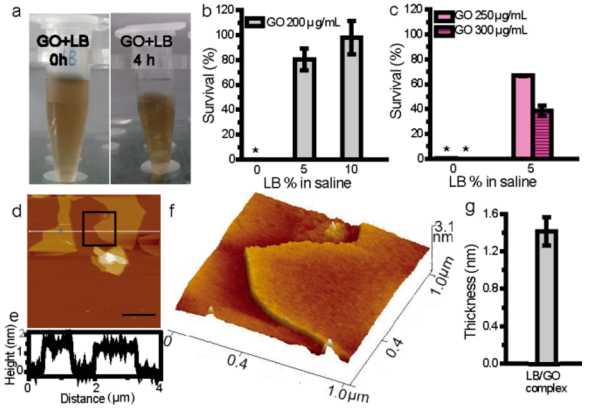

Figure 2. GO dispersion in LB-supplemented saline and related characterizations. (a) Photographs of GO dispersion at 200 μg/mL in saline supplemented with 5% LB broth before (left) and after (right) standing still for 4 h. Killing assays using (b) GO sheets of 200 μg/mL in saline, saline supplemented with 5% LB, and saline supplemented with 10% LB and (c) GO sheets of 250 and 300 μg/mL in saline supplemented with 5% LB. Controls are samples assayed in comparable ways but in unmodified saline. The *E. coli* inoculation level was consistently ~5×10^5 cfu/mL. Asterisks indicate bacterial survival percentage of <1%. Data points are reported as mean ± standard deviation. (d) A representative AFM image of GO sheets which were dispersed in LB-supplemented saline (5% LB broth) and subsequently washed to remove excess LB components and the corresponding (e) height and (f) three-dimensional profiles. Scale bar = 1 μm. (g) On the basis of the height profiles of AFM images, LB-masked GO sheets in saline supplemented with 5% LB exhibited an average sheet thickness of 1.41 ± 0.15 nm (averaged over eight individual sheets). Data points are reported as mean ± standard deviation.

Intriguingly, killing assays showed that, in saline supplemented with 10% LB broth, GO sheets of 80 and 200 μg/mL led to bacterial survival percentages of 101.9% and 97.95%, respectively (Figures 2b and S4, Supporting Information), indicating that the presence of only 10% LB broth in saline was enough to completely inactivate the bactericidal activity of ⩽200 μg/mL GO sheets. Similar results were observed in modified saline containing 5% LB broth, in which GO sheets of 80 and 200 μg/mL resulted in bacterial survival percentages of 102.2% and 80.4%, respectively (Figures 2b and S4, Supporting Information); in this case, the bactericidal activity of 200 μg/mL GO sheets was slightly recovered, suggesting that the relative dosage of GO versus LB may play a role in the deactivation. Thus, we speculated that increasing GO dose may help GO recover its bactericidal activity. Indeed, this was the case. In saline supplemented with 5% LB broth, GO sheets of 250 and 300 μg/mL—two doses capable of killing >99% of treated bacterial cells in saline—resulted in bacterial survival percentages of 66.9% and 38.6%, respectively (Figure 2c). Note that, in a plate killing assay, each zero-dilution well was initially inoculated to achieve ~5×10^5 cfu/mL. After 3 h incubation, those in LB-modified saline achieved ≥4×10^7 cfu/mL—corresponding to ~100-fold growth—irrespective of the presence or absence of GO (Figure S5, Supporting Information). Thus, GO's loss of bactericidal property and the concurrent bacterial growth observed in LB-supplemented saline may explain the prior observations that bacterial growth occurred in the presence of GO as determined by both inhibition assays and bacterial genomic DNA quantifications using GO in LB broth.[17]

The fact that the GO's antibacterial activity is related to the amount of LB broth suggests that one or more components of the broth are interacting with the GO in a way that quenches its activity. It is known that GO basal planes readily adsorb a variety of molecules via noncovalent interactions, a property extensively explored for biomedical applications.[4−6,22−28] Moreover, recent computer simulations suggested that GO sheets may destructively extract phospholipids from the bacterial cellular membranes onto their basal planes, leading to bacterial death.[10]

We hence hypothesized that the basal planes of GO may be crucial for its antibacterial activity and masking them by noncovalent adsorption of certain LB nutrients may account for its loss of antibacterial property in the presence of LB broth. The results of our initial studies were consistent with this hypothesis. Under AFM, GO dispersion in LB-supplemented saline (5% LB broth) retained the sheetlike morphology (Figure S6a, Supporting Information) of bare GO sheets in saline (Figure 1b) but exhibited an average sheet thickness of 1.58 ± 0.14 nm ($n = 2$, Figure S6d, Supporting Information), approximately 60% thicker than that of bare GO sheets in saline (1.00 ± 0.13 nm, Figure 1e), indicative of the presence of certain LB components on GO basal planes. Unfortunately, the presence of excess LB components and their aggregations made it difficult to move the AFM tip over the sample and obtain more AFM images necessary for further analysis. To remove excess LB components and their aggregations, we centrifuged and redispersed the LB/GO complexes in saline (details in the Supporting Information); the resultant dispersion appeared to be clear and light brown in color when freshly prepared but precipitated after standing still for 4 h (Figure S7b, Supporting Information). Under AFM, the redispersed LB/GO complexes retained the sheetlike morphology but exhibited an average sheet thickness of 1.41 ± 0.15 nm ($n = 8$, Figure 2g), close to that of GO in LB-supplemented saline (Figure S6d, Supporting Information) but significantly larger than that of bare GO (1.00 ± 0.13 nm, Figure 1e) ($p < 0.01$). Although the increase in sheet thickness is consistent with the presence of significant adsorbate on the GO basal planes, the LB extract is complex and the exact identity of the adsorbed species is currently

unknown. As such, we undertook a study using well-defined adsorbates.

BSA is a protein that GO basal planes readily adsorb via noncovalent adsorptions.[29] Using BSA as a model adsorbate, we assessed whether BSA−GO adsorption deactivates the bactericidal activity of GO. BSA−GO adsorption assays revealed that, when BSA adsorption saturated GO, the mass ratio of adsorbed BSA and GO, $BSA_{adsorbed}$:GO, varied slightly around 1:1 (Figure S8b, Supporting Information), consistent with previous studies.[29,30] Hence we used BSA_{total}:GO = 2:1 to ensure saturation of BSA−GO adsorption for all the following BSA-related experiments, unless specified otherwise. Freshly prepared GO dispersion (200 μg/mL) in BSA-supplemented saline (400 μg/mL BSA) appeared to be clear and light brown, but slight agglomeration occurred after standing still for 4 h (Figure 3a), similar as GO in LB-modified saline. The BSA−GO adsorption was also confirmed with zeta-potential measurements, as indicated by the less negative zeta-potential for GO in BSA-supplemented saline than that of bare GO sheets (Figure S9, Supporting Information). Under AFM, GO in BSA-supplemented saline clearly aggregated, but the thinnest area of the aggregations retained the sheetlike morphology (Figure S10a-c, Supporting Information) and exhibited an average sheet thickness of 4.74 ± 0.49 nm (n = 18, Figure S10d, Supporting Information). To improve the dispersity of the BSA-coated GO sheets, we centrifuged and redispersed the BSA/GO complexes in saline; the resultant dispersion appeared to be clear and light brown when prepared fresh but obviously precipited after standing still for 4 h (Figure S7c, Supporting Information), similar to the behavior of LB/GO complexes in saline (Figure S7b, Supporting Information). Under AFM, the redispersed BSA/GO complexes retained the sheetlike morphology (Figure 3b,c) but exhibited an average sheet thickness of 4.52 ± 0.52 nm (n = 10, Figure 3e), close to that of GO in BSA-supplemented saline (Figure S10d, Supporting Information) but significantly larger than that of uncoated GO (1.00 ± 0.13 nm, Figure 1e) (p < 0.01). Note that BSA has a molecular size of ∼14 nm × 4 nm × 4 nm.[29] Assuming that BSA does not denature upon adsorption, the as-observed average sheet thickness of BSA-saturated GO sheets corresponds to the sum of the thicknesses of a single GO sheet and that of an adsorbed BSA monolayer, which suggests that BSA may adsorb evenly and form a monolayer over the basal planes of a GO sheet.

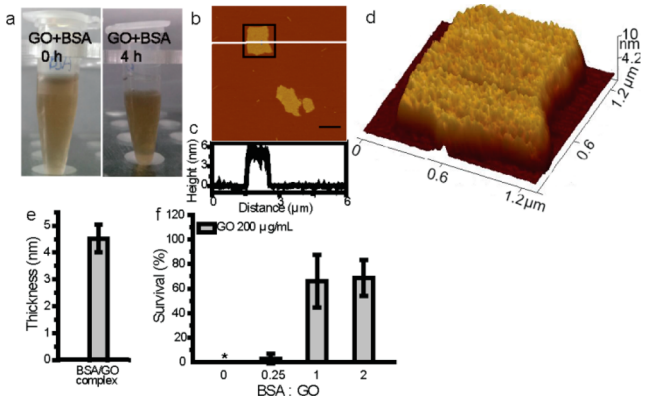

Figure 3. (a) Photographs of 200 μg/mL GO dispersion in BSA-supplemented saline (400 μg/mL BSA) before (left) and after (right) standing still for 4 h. (b) A representative AFM image of BSA-coated GO sheets (BSA:GO = 2:1) and the corresponding (c) height and (d) three-dimensional profiles. Scale bar = 1 μm. (e) On the basis of the height profiles of AFM images, BSA-saturated GO sheets exhibited an average sheet thickness of 4.52 ± 0.52 nm (averaged over 10 individual sheets). (f) Killing assays using 200 μg/mL GO dispersions in BSA-supplemented saline with varying BSA:GO mass ratios. Comparable assays using 200 μg/mL GO dispersions in unmodified saline were included for comparisons. The *E. coli* inoculation level was consistently ∼5 × 10^5 cfu/mL. Data points are reported as mean ± standard deviation. An asterisk indicates bacterial survival percentage of <1%.

We estimated that the adsorbed BSA molecules occupy approximately 56−84% of the GO basal plane area when BSA−GO adsorption saturates (BSA:GO = 1:1). Our estimation assumed a Brunauer−Emmett−Teller (BET) surface area of 600−900 m^2/g for GO,[31] and our estimated percentage is close to that reported by a prior study that estimated the maximal percent of GO basal plane area occupied by adsorbed BSA to be 43% by assuming a BET surface area of 900 m^2/g for GO.[29] Though formation of a BSA-multilayer could occur, little evidence was found to support its formation, as only extremely small areas on a very few BSA-saturated GO sheets were observed to exhibit an average sheet thickness other than ∼4.52 nm.

To assess whether the noncovalent adsorption of BSA on GO basal planes deactivates GO's bactericidal activity as hypothesized, we freshly prepared GO dispersion in BSA-supplemented saline prior to bacterial exposure and performed the same killing assays as those conducted in unmodified saline. These assays showed that, upon BSA supplementation in saline, GO partially lost its bactericidal activity and the degree of such inactivation varied depending on the amount of BSA supplemented (Figure 3f). In saline supplemented with BSA above BSA:GO saturation ratio (BSA_{total}:GO ≥ 1:1), 200 μg/mL GO sheets at BSA_{total}:GO = 2:1 and 1:1 led to bacterial survival percentages of 68.6% and 66.1%, respectively. In striking contrast, GO at the same dose in saline supplemented with BSA below the BSA:GO saturation ratio (BSA_{total}:GO = 0.25:1, 4-fold lower than that at saturation) led to a bacterial survival percentage of only 3%. Note that BSA itself in saline imposed no significant impact on bacterial viability up to 0.6 mg/mL (Figure S11, Supporting Information), the highest BSA concentration we used to pretreat GO. Taken together, these results indicate that GO basal planes are important action sites for its bactericidal property, consistent with previous computer simulations,[10] and masking them via noncovalent adsorption could significantly weaken the bactericidal activity of GO sheets.

A natural question that emerges is: why did the BSA-saturated GO sheets (at BSA_{total}:GO ≥ 1:1) still demonstrate residual bactericidal activity? The still sharp edges of GO sheets after BSA pretreatment and the inevitable void area left by 2D packing of BSA on GO basal planes represent two possible explanations, and we believe that the answer may be related to the latter. Considering the fact that BSA is a relatively large protein, its 2D packing may inevitably leave relatively large void areas on GO basal planes, which may be attributed to the observed residual bactericidal activity. If this was the case, switching to smaller adsorbate might help decrease such void areas on GO basal planes and, in doing so, lower the residual bactericidal activity of masked GO. To test this hypothesis, we used tryptophan (Trp)—an amino acid that GO basal planes readily adsorb[32]—as a model small adsorbate and examined how pretreating GO with Trp affects its bactericidal activity. Assuming compact 2D packing of tryptophan's indole group on

GO basal planes, we estimated that, at a mass ratio of Trp:GO = 6:1, an adsorbed tryptophan monolayer could occupy all the area of GO basal planes (details in the Supporting Information). To ensure saturation of Trp on GO, a mass ratio of Trp:GO = 12:1 was used for the following experiments, unless specified otherwise. Freshly prepared GO dispersion (200 μg/mL) in Trp-supplemented saline (2.4 mg/mL Trp) appeared to be clear and light brown but slight precipitation occurred after standing still for 4 h (Figure 4a), similar to the

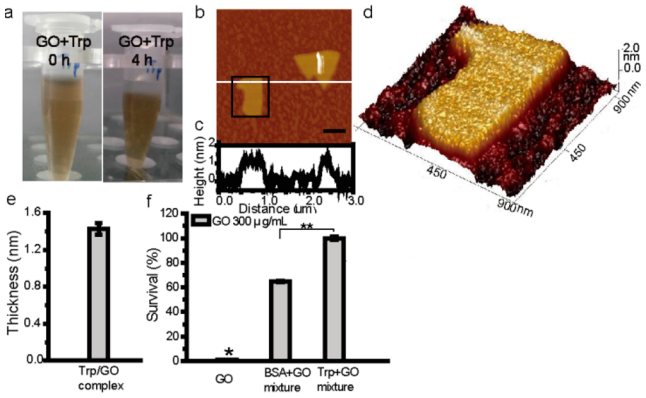

Figure 4. (a) Photographs of GO dispersion in saline supplemented with Trp, at mass ratio Trp:GO = 12:1, before (left) and after (right) standing still for 4 h. (b) A representative AFM image of Trp-saturated GO sheets in saline, at Trp:GO = 12:1, and the corresponding (c) height and (d) three-dimensional profiles. Scale bar = 0.5 μm. (e) On the basis of the height profiles of AFM images, Trp-saturated GO sheets exhibit an average sheet thickness of 1.42 ± 0.06 nm (averaged over seven individual sheets). (f) Killing assays using bare GO sheets, BSA-masked GO sheets (BSA:GO = 2:1), and Trp-masked GO (Trp:GO = 12:1); the same GO doses of 300 μg/mL are used. The *E. coli* inoculation level was consistently ~5 × 10^5 cfu/mL. Data points are reported as mean ± standard deviation. An asterisk indicates bacterial survival percentage of <1%. $^{**}p < 0.01$.

behavior of GO dispersions in both LB- and BSA-supplemented saline. Under AFM, GO sheets in Trp-supplemented saline aggregated slightly, but the very thin area of the aggregations retained similar sheet morphology to bare GO sheets (Figure S12a–c, Supporting Information) and exhibited an average sheet thickness of 1.40 ± 0.09 nm (n = 15, Figure S12d, Supporting Information). To improve the dispersity of Trp-adsorbed GO sheets, we centrifuged and redispersed the Trp/GO complex in saline; the dispersion appeared to be clear and light brown when freshly prepared but slightly precipited after standing still for 4 h (Figure S7d, Supporting Information), similar to the behavior of LB/GO complexes in saline (Figure S7b, Supporting Information). Under AFM, the redispersed Trp/GO complexes retained the sheetlike morphology of bare GO sheets (Figure 4b,c) but exhibited an average sheet thickness of 1.42 ± 0.06 nm (n = 7, Figure 4e), close to that of GO in Trp-supplemented saline (Figure S12d, Supporting Information) but significantly larger than that of bare GO sheets (1.00 ± 0.13 nm) ($p < 0.01$). Assuming that Trp adsorbs with its indole group lying parallel to GO basal planes, we estimated a thickness of the Trp monolayer to be approximately 0.4 nm high perpendicularly to GO basal planes. Thus, the as-observed average sheet thickness of Trp-saturated GO sheets corresponds to the sum of the thicknesses of a single GO sheet and that of an adsorbed Trp monolayer, verifying the adsorption of Trp over GO basal planes.

Now Trp does adsorb over GO basal planes, as did BSA. Would this significantly smaller adsorbate deactivate GO's bactericidal activity to significantly higher extent compared to BSA? This was indeed the case. Our killing assay results showed that, for GO sheets of 300 μg/mL, Trp-saturated ones (Trp:GO = 12:1) completely lost their bactericidal property and resulted in 100.1% bacterial survival, whereas BSA-saturated ones (BSA:GO = 2:1) were partially bactericidal, leading to a bacterial survival percentage of 64.7% (Figure 4f). Our control experiments showed that tryptophan itself in saline barely affected bacterial viability up to 3.66 mg/mL (Figure S13, Supporting Information), the highest Trp concentration we used to pretreat GO. Notably, Trp-unsaturated GO sheets (Trp:GO < 6:1) still partially retained the antibacterial activity of bare GO (Figure S14, Supporting Information). Combined with assays at varying BSA:GO (Figure 3f), these results indicate that the extent to which GO basal planes are masked by adsorbates—the availability of GO basal planes—determines the extent of deactivation of GO's bacterial activity.

Our bacterial killing assays evaluated bactericidal activity by counting visible colonies on agar plates, as normally done for a bactericidal assay. That GO treatment resulted in loss of a certain percentage of cfu/mL for the inoculated bacterial cells may have two possible explanations: GO is definitively bactericidal and indeed kills a significant percentage of inoculated bacterial cells or GO does not kill bacteria but simply renders a certain percentage of treated bacterial cells unable to form visible colonies on agar plates. To clarify which possibility is related with the answer, we performed bacterial dead/live viability assays. Both *E. coli* and *B. subtilis* (ATCC 6051) were used, considering that GO was reported to be bactericidal against both Gram-negative and -positive strains.[7] We briefly incubated the GO-treated bacteria with SYTO 9 and propidium iodide (PI)[33] and examined the staining effects under fluorescence microscopy. SYTO 9 is a cell-permeant green-fluorescent stain that labels both live and dead bacteria, whereas PI is a cell-impermeant red-fluorescent stain that only labels cells with compromised cellular membranes; both SYTO 9 and PI are nucleic acid stains. After brief incubation with SYTO 9 and PI, all GO-treated strains stained intensely red, indicative of dead cells (Figure 5). In contrast, strains treated similarly but without GO addition (i.e., control) were dark in the red channel, indicative of live cells (Figure 5). Combined with our killing assays, the bacterial dead/live viability assays showed that bare GO sheets indeed kill bacteria. Moreover, the effects of BSA- and Trp-adsorption on GO's bactericidal activity quantitatively assessed in classic plate killing assays were also qualitatively verified in the bacterial dead/live viability assays. Trp-saturated GO, which was completely inocuous in classic plate killing assays (Figure S14, Supporting Information), rendered treated bacterial strains dark in the red channel, like the untreated ones (Figure 5), indicative of live cells. In contrast, BSA-saturated GO, which led to a bacterial survival percentage of 68.6% in plate killing assays (Figure 3f), rendered treated bacterial strains stained intensely red, indicative of dead cells (Figure S15, Supporting Information); obviously, the qualitative nature of fluorescence-microscopy-based bacterial dead/live viability assays cannot differentiate survival percentages of <1% and ~60%. Taken together, our data suggest that bare GO sheets indeed kill bacteria and noncovalent adsorption

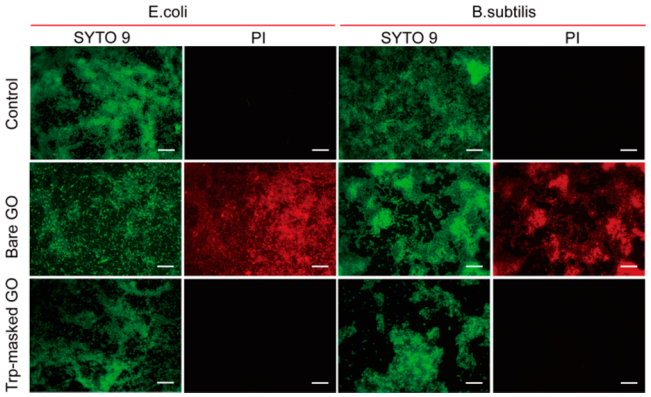

Figure 5. Representative fluorescence microscopy images of bacterial strains treated with bare GO and Trp-masked GO and subsequently stained briefly (15 min) with SYTO 9 (green) and PI (red). The treatment was carried out with bare GO sheets or Trp-masked GO sheets (Trp:GO = 12:1 to ensure saturation) for 15 min in saline (0.9% NaCl); both cases had the same GO doses of 200 μg/mL. Controls are assayed similarly but without the addition of GO or Trp-saturated GO. Scale bar = 20 μm.

on its basal planes deactivats its bactericidal activty to a varying extent depending on adsorbate used.

It should be noted that Trp, but not BSA, can be used as a sole carbon source for growth by *E. coli*. Is it possible that the similarities between Trp and LB, but not with BSA, simply originate in that bacteria are able to grow in the presence of Trp and LB, but not BSA? To exclude this possibility, we compared the cfu/mL counts for samples in related killing assays. After 3 h incubation, GO sheets in both Trp- and BSA-supplemented saline resulted in <2-fold increase in bacterial cfu/mL counts compared to bacterial inoculum size (Figure S16, Supporting Information), whereas those in LB-supplemented saline led to ~100-fold increase in cfu/mL counts (Figure S5, Supporting Information); bacterial inoculums sizes were consistently ~5 × 10^5 cfu/mL. Therefore, the as-observed similarities between the impact of Trp and LB, but not BSA, on GO's antibacterial property may originate in their similar capability of masking the GO basal planes, rather than their similarities in supporting bacterial growth.

Several possible antibacterial mechanisms were previously proposed for GO, including membrane stress, oxidative stress independent of reactive oxygen species (ROS), and nutrient deprivation imposed by GO's adherence.[7,9,10,12,34] For membrane stress, two possible action sites on GO were suggested: GO's sharp edges, which may act as "cutters" to disrupt the bacterial cellular membranes and cause leakage of intracellular substances such as RNA,[7,9] and GO's basal planes, which may contribute, for example, by destructively extracting membrane lipids.[10,12] Our results suggest that, to kill bacteria, GO relies heavily on the availability of its basal planes, where a variety of antibacterial processes such as membrane stress, oxidative stress, and even nutrient deprivation could occur. Our results clearly showed that membrane permeabilization is indisputably involved in the antibacterial activity of GO (Figure 5); additional studies are needed to establish the detailed mechanism.

Finally, we noted that the roles played by GO basal planes in its antibacterial activity could be extrapolated to its cytotoxicity against mammalian cells. Similar to the case of antibacterial property, controversial observations were reported for GO's cytotoxicity against mammalian cells. Some reports showed that GO has concentration-dependent cytotoxicity,[8,30,35] whereas others showed that GO has no obvious cytotoxicity or only slight cytotoxicity at high concentrations.[36] Such differing cytotoxicity of GO was previously attributed to fetal bovine serum (FBS), a protein-rich mixture normally supplemented in cell culture media.[30] Here, to examine how noncovalent adsorption on GO basal planes affects its cytotoxicity, we used HepG2 cells as representative mammalian cells and performed similar dead/live viability assays as in the case of bacteria. After brief incubation with SYTO 9 and PI, HepG2 cells treated with bare GO sheets stained intensely red, indicative of dead cells (Figure 6), whereas those treated with

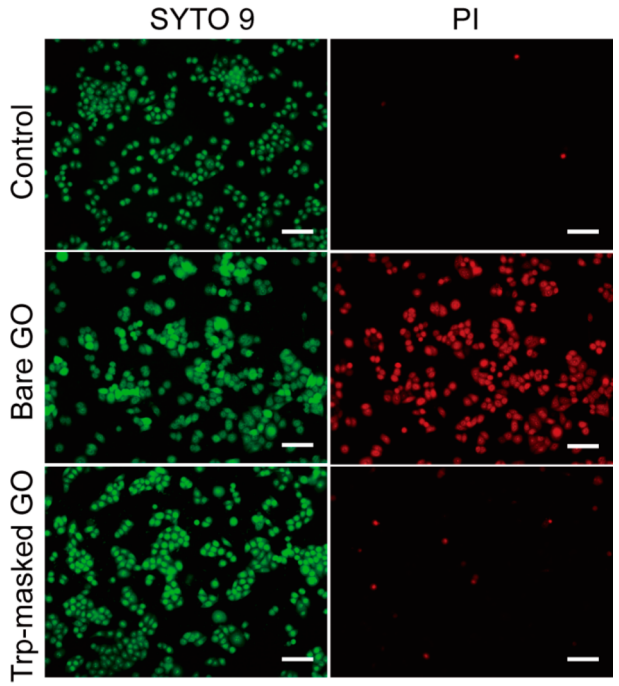

Figure 6. Representative fluorescence microscopy images of HepG2 cells treated with bare GO sheets and Trp-masked GO sheets and subsequently stained briefly (15 min) with SYTO 9 (green) and PI (red). The cell treatment was carried out with bare GO sheets or Trp-masked GO sheets (mass ratio Trp:GO = 12:1 to ensure saturation) for 15 min in sterile saline (0.9% NaCl); GO doses in both cases were set the same at 200 μg/mL. Controls were assayed similarly but without addition of GO or Trp-saturated GO. Scale bar = 100 μm.

Trp-masked GO sheets (Figure 6) as well as those treated with BSA-saturated GO (Figure S17, Supporting Information) were mostly dark in the red channel, like the control, indicative live cells. Clearly, bare GO is cytotoxic to mamallian cells and noncovalent adsorption on its basal planes attenuated its cytotoxicity. Similar attenuation of GO's cytotoxicity was also observed in both Dulbecco's modified Eagle's medium (DMEM) and FBS-supplemented DMEM (Figure S17, Supporting Information), media rich in amino acids/proteins, consistent with prior study[30] and also similar to GO's loss of antibacterial activity in LB broth. Taken together, these observations suggest that bare GO sheets are intrinsically cytotoxic to mammalian cells and noncovalent adsorption on GO basal planes deactivates GO's cytotoxicity, indicative of a global deactivation mechanism for GO's cytotoxicity against both bacteria and mammalian cells.

CONCLUSION

In summary, we have systematically studied whether GO is intrinsically antibacterial and, if that is the case, why it appeared to be inactive under certain conditions. Our results revealed that bare GO indeed kills bacteria and that masking its basal planes via noncovalent adsorption renders GO inactive against bacteria, which may explain GO's loss of antibacterial activity as previously observed in antibacterial assays performed in LB broth and also suggests that the availability of GO basal planes determines GO's antibacterial activity. Our study explains the contradictory results on GO's antibacterial activity in the literature and defines the necessary parameters for achieving the optimal bactericidal activity of GO. Moreover, we also showed that bare GO is cytotoxic to mammalian cells and masking its basal planes via noncovalent adsorption also largely attenuates its cytotoxicity, using a qualitative cell viability assay technique. Taken together, the results presented here show that the availability of GO basal planes may be a global key factor determining GO's cytotoxicity against both bacteria and mammalian cells.

ASSOCIATED CONTENT

Supporting Information

Results on the GtO preparation and subsequent thermogravimetric and FT-IR analysis, additional killing assays, BSA calibration curve measurements, and BSA−GO adsorption measurements, zeta-potential measurements, and dead/live kit assays. This material is available free of charge via the Internet at http://pubs.acs.org.

AUTHOR INFORMATION

Corresponding Authors

*H.L.: e-mail, hliu@pitt.edu; phone, +1(412)624-2062.

*L.Y.: e-mail, lhyang@ustc.edu.cn; phone, +86(551) 6360 6960.

Author Contributions

#The manuscript was written through contributions of all authors. All authors have given approval to the final version of the manuscript. J.-G.P., J.A., and K.H. contributed equally.

Notes

The authors declare no competing financial interest.

ACKNOWLEDGMENTS

The authors thank Prof. Shiyong Liu for help on zeta-potential measurements, and Jianliu Huang for AFM characterizations. L.Y. gratefully acknowledges support from the NSFC (11074178, 21174138), Ministry of Education of China (NCET-13-0547, FRF for CU WK2060140008 and WK2060200012), and Anhui Provincial Natural Science Foundation (1308085QB28). H.L. acknowledges additional support from AFOSR (FA9550-13-1-0083) and ONR (N000141310575).

REFERENCES

(1) Geim, A. K. Graphene: Status and Prospects. *Science* **2009**, *324*, 1530−1534.

(2) Novoselov, K. S.; Falko, V. I.; Colombo, L.; Gellert, P. R.; Schwab, M. G.; Kim, K. A Roadmap for Graphene. *Nature* **2012**, *490*, 192−200.

(3) He, H.; Klinowski, J.; Forster, M.; Lerf, A. A New Structural Model for Graphite Oxide. *Chem. Phys. Lett.* **1998**, *287*, 53−56.

(4) Bitounis, D.; Ali-Boucetta, H.; Hong, B. H.; Min, D.-H.; Kostarelos, K. Prospects and Challenges of Graphene in Biomedical Applications. *Adv. Mater.* **2013**, *25*, 2258−2268.

(5) Chung, C.; Kim, Y.-K.; Shin, D.; Ryoo, S.-R.; Hong, B. H.; Min, D.-H. Biomedical Applications of Graphene and Graphene Oxide. *Acc. Chem. Res.* **2013**, *46*, 2211−2224.

(6) Feng, L.; Wu, L.; Qu, X. New Horizons for Diagnostics and Therapeutic Applications of Graphene and Graphene Oxide. *Adv. Mater.* **2013**, *25*, 168−186.

(7) Akhavan, O.; Ghaderi, E. Toxicity of Graphene and Graphene Oxide Nanowalls against Bacteria. *ACS Nano* **2010**, *4*, 5731−5736.

(8) Hu, W.; Peng, C.; Luo, W.; Lv, M.; Li, X.; Li, D.; Huang, Q.; Fan, C. Graphene-Based Antibacterial Paper. *ACS Nano* **2010**, *4*, 4317−4323.

(9) Liu, S.; Zeng, T. H.; Hofmann, M.; Burcombe, E.; Wei, J.; Jiang, R.; Kong, J.; Chen, Y. Antibacterial Activity of Graphite, Graphite Oxide, Graphene Oxide, and Reduced Graphene Oxide: Membrane and Oxidative Stress. *ACS Nano* **2011**, *5*, 6971−6980.

(10) Tu, Y.; Lv, M.; Xiu, P.; Huynh, T.; Zhang, M.; Castelli, M.; Liu, Z.; Huang, Q.; Fan, C.; Fang, H.; Zhou, R. Destructive Extraction of Phospholipids from *Escherichia coli* Membranes by Graphene Nanosheets. *Nat. Nanotechnol.* **2013**, *8*, 594−601.

(11) Gurunathan, S.; Han, J. W.; Dayem, A. A.; Eppakayala, V.; Kim, J. H. Oxidative Stress-Mediated Antibacterial Activity of Graphene Oxide and Reduced Graphene Oxide in *Pseudomonas aeruginosa*. *Int. J. Nanomed.* **2012**, *7*, 5901−5914.

(12) Liu, S.; Hu, M.; Zeng, T. H.; Wu, R.; Jiang, R.; Wei, J.; Wang, L.; Kong, J.; Chen, Y. Lateral Dimension-Dependent Antibacterial Activity of Graphene Oxide Sheets. *Langmuir* **2012**, *28*, 12364−12372.

(13) Chen, J.; Peng, H.; Wang, X.; Shao, F.; Yuan, Z.; Han, H. Graphene Oxide Exhibits Broad-Spectrum Antimicrobial Activity against Bacterial Phytopathogens and Fungal Conidia by Intertwining and Membrane Perturbation. *Nanoscale* **2014**, *6*, 1879−1889.

(14) Park, S.; Mohanty, N.; Suk, J. W.; Nagaraja, A.; An, J.; Piner, R. D.; Cai, W.; Dreyer, D. R.; Berry, V.; Ruoff, R. S. Biocompatible, Robust Free-Standing Paper Composed of a Tween/Graphene Composite. *Adv. Mater.* **2010**, *22*, 1736−1740.

(15) Tang, J.; Chen, Q.; Xu, L.; Zhang, S.; Feng, L.; Cheng, L.; Xu, H.; Liu, Z.; Peng, R. Graphene Oxide−Silver Nanocomposite as a Highly Effective Antibacterial Agent with Species-Specific Mechanisms. *ACS Appl. Mater. Interfaces* **2013**, *5*, 3867−3874.

(16) Tian, T.; Shi, X.; Cheng, L.; Luo, Y.; Dong, Z.; Gong, H.; Xu, L.; Zhong, Z.; Peng, R.; Liu, Z. Graphene-Based Nanocomposite as an Effective, Multifunctional, and Recyclable Antibacterial Agent. *ACS Appl. Mater. Interfaces* **2014**, *6*, 8542−8548.

(17) Ruiz, O. N.; Fernando, K. A. S.; Wang, B.; Brown, N. A.; Luo, P. G.; McNamara, N. D.; Vangsness, M.; Sun, Y.-P.; Bunker, C. E. Graphene Oxide: A Nonspecific Enhancer of Cellular Growth. *ACS Nano* **2011**, *5*, 8100−8107.

(18) Veerapandian, M.; Zhang, L.; Krishnamoorthy, K.; Yun, K. Surface Activation of Graphene Oxide Nanosheets by Ultraviolet Irradiation for Highly Efficient Anti-Bacterials. *Nanotechnology* **2013**, *24*, 395706.

(19) Wang, G.; Qian, F.; Saltikov, C.; Jiao, Y.; Li, Y. Microbial Reduction of Graphene Oxide by Shewanella. *Nano Res.* **2011**, *4*, 563−570.

(20) Hummers, W. S.; Offeman, R. E. Preparation of Graphitic Oxide. *J. Am. Chem. Soc.* **1958**, *80*, 1339−1339.

(21) Hirata, M.; Gotou, T.; Horiuchi, S.; Fujiwara, M.; Ohba, M. Thin-Film Particles of Graphite Oxide. 1: High-Yield Synthesis and Flexibility of the Particles. *Carbon* **2004**, *42*, 2929−2937.

(22) Some, S.; Ho, S.-M.; Dua, P.; Hwang, E.; Shin, Y. H.; Yoo, H.; Kang, J.-S.; Lee, D.-k.; Lee, H. Dual Functions of Highly Potent Graphene Derivative—Poly-L-lysine Composites to Inhibit Bacteria and Support Human Cells. *ACS Nano* **2012**, *6*, 7151−7161.

(23) Tian, B.; Wang, C.; Zhang, S.; Feng, L.; Liu, Z. Photothermally Enhanced Photodynamic Therapy Delivered by Nano-Graphene Oxide. *ACS Nano* **2011**, *5*, 7000−7009.

(24) Chou, S. S.; De, M.; Luo, J.; Rotello, V. M.; Huang, J.; Dravid, V. P. Nanoscale Graphene Oxide (NGO) as Artificial Receptors: Implications for Biomolecular Interactions and Sensing. *J. Am. Chem. Soc.* **2012**, *134*, 16725−16733.
(25) Shi, X.; Gong, H.; Li, Y.; Wang, C.; Cheng, L.; Liu, Z. Graphene-Based Magnetic Plasmonic Nanocomposite for Dual Bioimaging and Photothermal Therapy. *Biomaterials* **2013**, *34*, 4786−4793.
(26) Wang, Y.; Wang, K.; Zhao, J.; Liu, X.; Bu, J.; Yan, X.; Huang, R. Multifunctional Mesoporous Silica-Coated Graphene Nanosheet Used for Chemo-Photothermal Synergistic Targeted Therapy of Glioma. *J. Am. Chem. Soc.* **2013**, *135*, 4799−4804.
(27) Liu, Z.; Robinson, J. T.; Sun, X.; Dai, H. Pegylated Nanographene Oxide for Delivery of Water-Insoluble Cancer Drugs. *J. Am. Chem. Soc.* **2008**, *130*, 10876−10877.
(28) Li, M.; Yang, X.; Ren, J.; Qu, K.; Qu, X. Using Graphene Oxide High near-Infrared Absorbance for Photothermal Treatment of Alzheimer's Disease. *Adv. Mater.* **2012**, *24*, 1722−1728.
(29) Mu, Q.; Su, G.; Li, L.; Gilbertson, B. O.; Yu, L. H.; Zhang, Q.; Sun, Y.-P.; Yan, B. Size-Dependent Cell Uptake of Protein-Coated Graphene Oxide Nanosheets. *ACS Appl. Mater. Interfaces* **2012**, *4*, 2259−2266.
(30) Hu, W.; Peng, C.; Lv, M.; Li, X.; Zhang, Y.; Chen, N.; Fan, C.; Huang, Q. Protein Corona-Mediated Mitigation of Cytotoxicity of Graphene Oxide. *ACS Nano* **2011**, *5*, 3693−3700.
(31) McAllister, M. J.; Li, J.-L.; Adamson, D. H.; Schniepp, H. C.; Abdala, A. A.; Liu, J.; Herrera-Alonso, M.; Milius, D. L.; Car, R.; Prud'homme, R. K.; Aksay, I. A. Single Sheet Functionalized Graphene by Oxidation and Thermal Expansion of Graphite. *Chem. Mater.* **2007**, *19*, 4396−4404.
(32) Zhang, M.; Yin, B.-C.; Wang, X.-F.; Ye, B.-C. Interaction of Peptides with Graphene Oxide and Its Application for Real-Time Monitoring of Protease Activity. *Chem. Commun.* **2011**, *47*, 2399−2401.
(33) Rapireddy, S.; Nhon, L.; Meehan, R. E.; Franks, J.; Stolz, D. B.; Tran, D.; Selsted, M. E.; Ly, D. H. Rtd-1mimic Containing γ_{PNA} Scaffold Exhibits Broad-Spectrum Antibacterial Activities. *J. Am. Chem. Soc.* **2012**, *134*, 4041−4044.
(34) Akhavan, O.; Ghaderi, E. *Escherichia coli* Bacteria Reduce Graphene Oxide to Bactericidal Graphene in a Self-Limiting Manner. *Carbon* **2012**, *50*, 1853−1860.
(35) Zhang, Y.; Ali, S. F.; Dervishi, E.; Xu, Y.; Li, Z.; Casciano, D.; Biris, A. S. Cytotoxicity Effects of Graphene and Single-Wall Carbon Nanotubes in Neural Phaeochromocytoma-Derived Pc12 Cells. *ACS Nano* **2010**, *4*, 3181−3186.
(36) Chang, Y.; Yang, S.-T.; Liu, J.-H.; Dong, E.; Wang, Y.; Cao, A.; Liu, Y.; Wang, H. In Vitro Toxicity Evaluation of Graphene Oxide on A549 Cells. *Toxicol. Lett.* **2011**, *200*, 201−210.